

Numerical Analysis of Specific Absorption Rate and Heat Transfer in Human Head Subjected to Mobile Phone Radiation: Effects of User Age and Radiated Power

Teerapot Wessapan
Phadungsak Rattanadecho
e-mail: ratphadu@engr.tu.ac.th

Research Center of Microwave Utilization in
Engineering (RCME),
Department of Mechanical Engineering,
Faculty of Engineering,
Thammasat University, Rangsit Campus,
Pathumthani 12120, Thailand

The human head is one of the most sensitive parts of the human entire body when exposed to electromagnetic radiation. This electromagnetic radiation interacts with the human head and may lead to detrimental effects on human health. However, the resulting thermophysiological response of the human head is not well understood. In order to gain insight into the phenomena occurring within the human head with temperature distribution induced by electromagnetic field, a detailed knowledge of absorbed power distribution as well as temperature distribution is necessary. This study presents a numerical analysis of specific absorption rate and heat transfer in the heterogeneous human head model exposed to mobile phone radiation. In the heterogeneous human head model, the effects of user age and radiated power on distributions of specific absorption rate and temperature profile within the human head are systematically investigated. This study focuses attention on organs in the human head in order to investigate the effects of mobile phone radiation on the human head. The specific absorption rate and the temperature distribution obtained by numerical solution of electromagnetic wave propagation and unsteady bioheat transfer equation in various tissues in the human head during exposure to mobile phone radiation are presented. [DOI: 10.1115/1.4006595]

Keywords: microwave, temperature distribution, specific absorption rate, human head, heat transfer

1 Introduction

As a result of the enormous increase in mobile phone usage throughout the world, the effect of mobile phone radiation on human health has become the subject of recent interest and study. In recent years, there is an increasing public concern about the health implications of the use of mobile phones. This concern is heightened when the power absorption in the brain and the sensation of warmth for the ear and skin in close proximity to the telephone induce temperature increase inside it.

For this reason, various public organizations in the world have established safety guidelines for electromagnetic wave absorption [1,2]. For electromagnetic wave exposures, these guidelines are based on peak specific absorption rate (SAR). The power absorption of electromagnetic energy in human tissues induces temperature increases inside tissue. Although the safety standards are regulated in terms of the peak SAR value of tissue, the maximum temperature increase in the human head caused by electromagnetic energy absorption is an actual influence of the dominant factors that induce adverse physiological effects. The severity of the physiological effect produced by small temperature increases can be expected to worsen in sensitive organs. Actually, a small temperature increase in the brain of 3.5 °C is noted to be an allowable limit which does not lead to physiological damage [3].

Additionally, it is reported that a very small temperature increase in the hypothalamus of 0.2–0.3 °C leads to altered thermoregulatory behavior [4].

Some significant thermal damage can occur in sensitive organs under conditions of partial body exposure to intense electromagnetic waves. Mobile phones are electromagnetic radiation devices, which may be harmful to human health from their radiation. Thus, it is interesting to analyze the heat transfer in the human head due to electromagnetic wave exposures. In accordance with the development of the computer and numerical analysis techniques, an anatomical human head model can be incorporated into simulated studies.

Recently, the modeling of heat transport in human tissue has been investigated. Pennes' bioheat equation, introduced by Pennes [5] based on the heat diffusion equation, is frequently used for analysis of heat transfer in human tissues. The studies of high temperature tissue ablation using a modified bioheat equation to include tissue internal water evaporation during heating have been proposed [6]. The simulation result is found in agreement with experimental results. Okajima et al. [7] derived the dimensionless steady-state solutions of the bioheat transfer equation to discuss the bioheat transfer characteristics common to all organs or tissue. Chua and Chou [8] have developed a bioheat model to study the freeze-thaw thermal process of cryosurgery. The topic of temperature increases in human tissue caused by exposure to electromagnetic waves has been of interest for several years [9]. The studies have been conducted using the coupled model of the bioheat equation and electromagnetic wave equation [10–13]. In the past, the experimental data on the correlation of SAR levels to the

Contributed by the Heat Transfer Division of ASME for publication in the JOURNAL OF HEAT TRANSFER. Manuscript received April 11, 2011; final manuscript received April 9, 2012; published online October 5, 2012. Assoc. Editor: Darrell W. Pepper.

temperature increases in the human head are sparse. Most previous studies of a human exposed to an electromagnetic field were mainly focused on SAR and electric field distributions. Nevertheless, they have not been considering heat transfer in their model during exposure to electromagnetic fields. That leads to an incomplete analysis. Therefore, to approach reality, modeling of heat transport in human tissue is must be cooperating with the modeling of electromagnetics in order to completely explain these interaction characteristics.

However, most studies of electromagnetic wave exposure to the human head have not considered a realistic domain with complicated organs of several types of tissue, and experimental validation is limited or nonexistent. There are few studies on the temperature and electromagnetic field interaction in a realistic physical model of the human head due to the complexity of the problem, even though it is directly related to thermal injury of tissue. Moreover, in general situations involving near-field exposures, it is well known that the exposure conditions, such as user age and radiated power, play an important role in electromagnetic energy absorption. Therefore, in order to provide information on levels of exposure and health effects from mobile phone radiation, it is essential to simulate both electromagnetic field and heat transfer within an anatomically based human head model to represent actual processes of heat transfer within the human head.

Our research group has tried to numerically investigate the temperature increase in human tissue subjected to electromagnetic fields in many problems, such as Wessapan et al. [11] carried out a numerical analysis of specific absorption rate and heat transfer in the human body to leakage electromagnetic field, Wessapan et al. [12] utilized a 2D finite element method to obtain the SAR and temperature increase in the human body exposed to electromagnetic waves, and Keangin et al. [13] carried out on the numerical simulation of liver cancer treated using the complete mathematical model considered the coupled model of electromagnetic wave propagation, heat transfer, and mechanical deformation in biological tissue in the couple way.

Recently, Wessapan et al. [10] carried out a numerical analysis of specific absorption rate and temperature distributions in the realistic human head model exposed to mobile phone radiation at 900 MHz and 1800 MHz. The effects of operating frequency and gap distance between the mobile phone and the human head on distributions of specific absorption rate and temperature profile within the human head were investigated. It was found that the maximum temperature increase in skin of 1800 MHz frequency is higher than that of 900 MHz frequency. While the maximum temperature increases in brain of 1800 MHz frequency are lower than that of 900 MHz frequency. A smaller gap distance between the mobile phone and the human head leads to higher electric field intensities, SAR, and heat generation inside the human head, thereby increasing the temperature within the human head.

The work described in this paper is substantially extended from our previous work [10] by further puts the focus on the effects of user age and radiated power. In this study, a three-dimensional human head model was used to simulate the SAR distribution and the temperature distribution over the human head at different geometry. Electromagnetic wave propagation in tissue was investigated by using Maxwell's equations. An analysis of heat transfer in human tissue exposed to electromagnetic waves was investigated by using the bioheat equation. The effects of user age (adult and 7 years old child) and radiated power (1.0, 1.5, and 2.0 W) on distributions of specific absorption rate and temperature profile within the human head are systematically investigated. The 900 MHz frequency was chosen for the simulations in this study, as it is a wavelength in the microwave band and is used frequently in the areas of cell phone usage. The obtained values provide an indication of limitations that must be considered for temperature increases due to electromagnetic energy absorption from mobile phones.

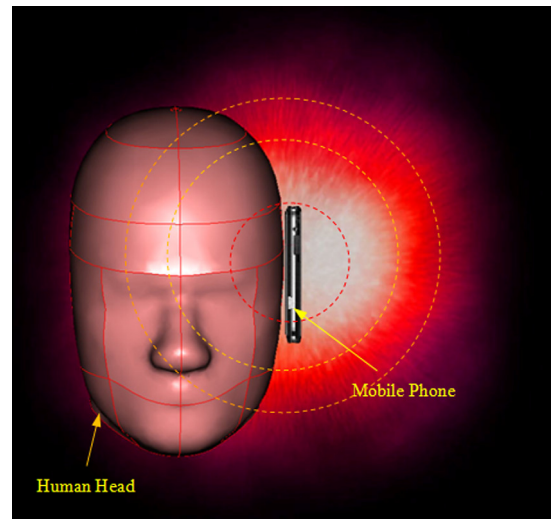


Fig. 1 Human head exposed to mobile phone radiation

2 Formulation of the Problem

Figure 1 shows the radiation of electromagnetic energy from a mobile phone to a heterogeneous human head model. Due to an ethical consideration, exposing a human to electromagnetic fields for experimental purposes is limited. It is more convenient to develop a realistic human head model through numerical simulation. In Sec. 3, an analysis of specific absorption rate and heat transfer in the layered human head exposed to mobile phone radiation will be illustrated. The system of governing equations as well as initial and boundary conditions is solved numerically using the finite element method via COMSOLTM MULTIPHYSICS.

3 Methods and Model

The first step in evaluating the effects of a certain exposure to radiation in the human head is the determination of the induced internal electromagnetic field and its spatial distribution. Thereafter, electromagnetic energy absorption which results in temperature increases within the human head and other interactions will be considered.

3.1 Physical Model. In this study, a patch antenna of a mobile phone located at the left side of a human head with a certain position is considered as a near-field radiation source for human head models. Figure 2(a) shows the three-dimensional human head model with the patch antenna used in this study. This model comprises four types of tissue including skin, fat, skull, and brain. These tissues have different dielectric and thermal properties. Figure 2(b) and Table 1 give adult and child head dimensions used in this study, which are directly taken from statistical body-size data [14]. The dielectric properties of tissues at the frequency of 900 MHz and thermal properties are given in Tables 2 and 3, respectively. There are insufficient data of thermal properties for children in the literature; therefore, there is no distinction between the adult and children.

3.2 Equations for Electromagnetic Wave Propagation Analysis. Mathematical models are developed to predict the electric field and SAR with relation to temperature gradients within the human head. To simplify the problem, the following assumptions are made:

- (1) Electromagnetic wave propagation is modeled in three dimensions.
- (2) The human head in which electromagnetic waves interact with the human head proceeds in free space.

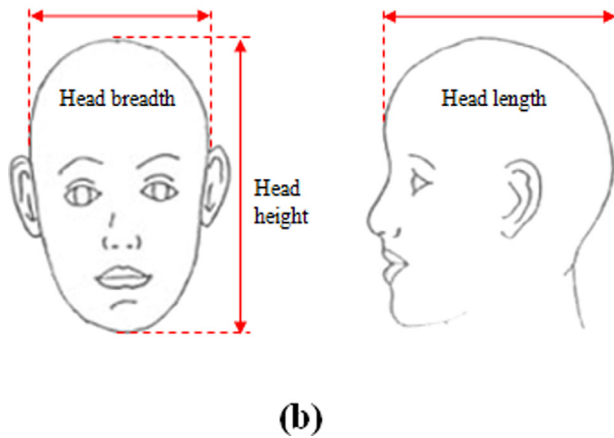
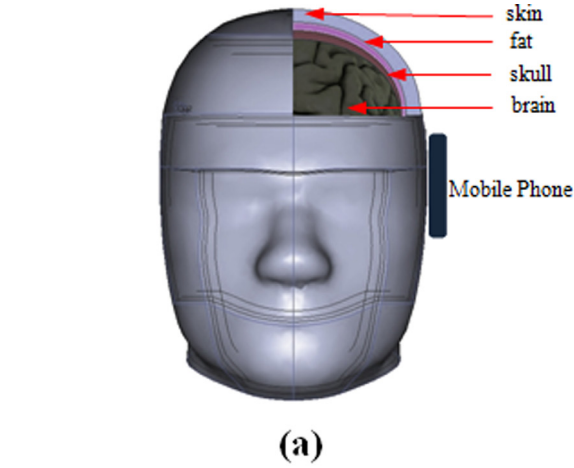


Fig. 2 Human head model. (a) Cross section human head model with mobile phone. (b) Dimensions of human head model.

- (3) The free space is truncated by a scattering boundary condition.
- (4) The model assumes that dielectric properties of each tissue are uniform and constant.

The electromagnetic wave propagation in a human head is calculated using Maxwell's equations [11,15], which mathematically describe the interdependence of the electromagnetic waves. The general form of Maxwell's equations is simplified to demonstrate the electromagnetic field penetrated in human head as the following equation:

$$\nabla \times \frac{1}{\mu_r} \nabla \times E - k_0^2 \epsilon_r E = 0 \quad (1)$$

where E is electric field intensity (V/m), μ_r is relative magnetic permeability, ϵ_r is relative dielectric constant, and k_0 is the free space wave number (m^{-1}).

3.2.1 Boundary Condition for Wave Propagation Analysis. Electromagnetic energy is emitted by the patch antenna and strikes the human head with a particular radiated power. The lumped port where it used to define a voltage drop across two patches is placed between the two patches at the bottom of the patch antenna in order to generate an electromagnetic field. Therefore, the boundary condition for solving electromagnetic wave propagation, as shown in Fig. 3, is described as follows:

Table 1 Head dimension used in this study [14]

	Adult (cm)	7 years old child (cm)
Head length	18.8	17.3
Head breadth	16	14.9
Head height	23.7	20.8

Table 2 Dielectric properties of tissues at 900 MHz [18]

Type of tissue	Adults		7 years old	
	ϵ_r	σ (S/m)	ϵ_r	σ (S/m)
Skin	41.41	0.87	42.47	0.89
Fat	11.33	0.11	12.29	0.12
Bone	20.79	0.34	21.97	0.36
Brain	45.805	0.765	46.75	0.78

Table 3 Thermal properties of tissues [11,19]

Tissue	ρ (kg/m^3)	k ($\text{W}/\text{m}^\circ\text{C}$)	C ($\text{J}/\text{kg}^\circ\text{C}$)	Q_{met} (W/m^3)	ω_b (1/s)
Skin	1125	0.42	3600	1620	0.02
Fat	916	0.25	3000	300	4.58×10^{-4}
Bone	1990	0.37	3100	610	4.36×10^{-4}
Brain	1038	0.535	3650	7100	8.83×10^{-3}

At the bottom of the patch antenna, an electromagnetic simulator employs lumped port boundary condition with specified radiated power

$$Z_{\text{in}} = \frac{V_1}{I_1} = \frac{E_1 l_1}{I_1} \quad (2)$$

where Z_{in} is the input impedance (Ω), V_1 is the voltage along the edges (V), I_1 is the electric current magnitude (A), E_1 is the electric field along the source edge (V/m), and l_1 is the edge length (m).

The patch of the antenna acts approximately as a cavity in which the perfect electric conductor on the inner and outer surfaces is assumed. Hence, the perfect-electric-conductor boundary condition along the patches on the antenna is considered

$$n \times E = 0 \quad (3)$$

Boundary conditions along the interfaces between different mediums, for example, between air and tissue or tissue and tissue, are considered as continuity boundary conditions

$$n \times (E_1 - E_2) = 0 \quad (4)$$

The outer sides of the calculated domain, i.e., free space, are considered as scattering boundary conditions [11]

$$n \times (\nabla \times E) - jkn \times (E \times n) = -n \times (E_0 \times jk(n-k)) \exp(-jk \cdot r) \quad (5)$$

where k is the wave number (m^{-1}), σ is the electric conductivity (S/m), n is the normal vector, $j = \sqrt{-1}$, and E_0 is the incident plane wave (V/m).

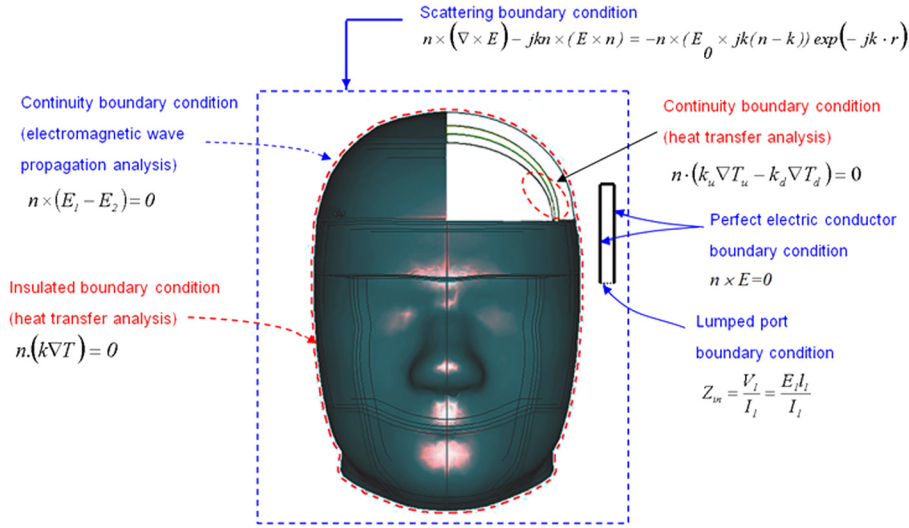


Fig. 3 Boundary condition for analysis of electromagnetic wave propagation and heat transfer

3.3 Interaction of Electromagnetic Waves and Human Tissue. Interaction of electromagnetic fields and biological tissue can be defined in terms of SAR. When electromagnetic waves propagate through the human tissue, the energy of electromagnetic wave propagation is absorbed by the tissue. The specific absorption rate is defined as power dissipation rate normalized by material density [11,16]. The specific absorption rate is given by

$$\text{SAR} = \frac{\sigma}{\rho} |E|^2 \quad (6)$$

3.4 Equations for Heat Transfer Analysis. To solve the thermal problem, the temperature distribution in the human head has been evaluated by the bioheat equation according to Maxwell's equations. The temperature distribution corresponds to the SAR. This is because the SAR within the human head distributes, owing to energy absorption. Thereafter, the absorbed energy is converted to thermal energy, which increases the tissue temperature.

Heat transfer analysis of the human head is modeled in three dimensions. To simplify the problem, the following assumptions are made:

- (1) Human tissue is biomaterial with uniform and constant thermal properties.
- (2) There is no phase change of substance within the tissue.
- (3) There is no energy exchange throughout the human head model.
- (4) There is no chemical reaction within the tissue.

The temperature distribution within the human head is obtained by solving Pennes' bioheat equation [11,17]. The transient bioheat equation describes effectively how heat transfer occurs within the human head, and the equation can be written as

$$\rho C \frac{\partial T}{\partial t} = \nabla \cdot (k \nabla T) + \rho_b C_b \omega_b (T_b - T) + Q_{\text{met}} + Q_{\text{ext}} \quad (7)$$

where ρ is the tissue density (kg/m^3), C is the heat capacity of tissue (J/kg K), k is the thermal conductivity of tissue (W/m K), T is the tissue temperature ($^{\circ}\text{C}$), T_b is the temperature of blood ($^{\circ}\text{C}$), ρ_b is the density of blood (kg/m^3), C_b is the heat capacity of blood (3960 J/kg K), ω_b is the blood perfusion rate ($1/\text{s}$), Q_{met} is the metabolism heat source (W/m^3), and Q_{ext} is the external heat source (electromagnetic heat-source density) (W/m^3).

In the analysis, heat conduction between tissue and blood flow is approximated by the blood perfusion term, $\rho_b C_b \omega_b (T_b - T)$.

The external heat source term is equal to the resistive heat generated by the electromagnetic field (electromagnetic power absorbed), which is defined as [11]

$$Q_{\text{ext}} = \frac{1}{2} \sigma_{\text{tissue}} |\bar{E}|^2 = \frac{\rho}{2} \cdot \text{SAR} \quad (8)$$

where $\sigma_{\text{tissue}} = 2\pi f \epsilon'' \epsilon_0$.

3.4.1 Boundary Condition for Heat Transfer Analysis. Heat transfer is considered only in the human head, which does not include parts of the surrounding space. As shown in Fig. 3, the outer surface of the human head corresponding to assumption (3) is considered to be a thermally insulated boundary condition

$$n \cdot (k \nabla T) = 0 \quad (9)$$

It is assumed that no contact resistant occurs between the internal organs of the human head. Therefore, the internal boundaries are assumed to be a continuous

$$n \cdot (k_u \nabla T_u - k_d \nabla T_d) = 0 \quad (10)$$

3.5 Calculation Procedure. In this study, the finite element method is used to analyze the transient problems. The computational scheme is to assemble a finite element model and compute a local heat generation term by performing an electromagnetic calculation using tissue properties. In order to obtain a good approximation, a fine mesh is specified in the sensitive areas. This study provides a variable mesh method for solving the problem as shown in Fig. 4. The model of bioheat equation and Maxwell's equation is then solved. All computational processes are implemented using COMSOLTM MULTIPHYSICS, to demonstrate the phenomena that occur within the human head exposed to electromagnetic field. The system of governing equations is solved with the unsymmetric multifrontal method. The electromagnetic power absorption at each point is computed and used to solve the time-dependent temperature distribution. All steps are repeated, until the required exposure time is reached. The calculation using time step for thermal model of 0.1 s and time step for electromagnetic field model of 10^{-11} s. The convergence criterion is specified at 10^{-6} and the maximum number of iterations is set to 1000 to assure that the transient solution is accurate. The 3D model is

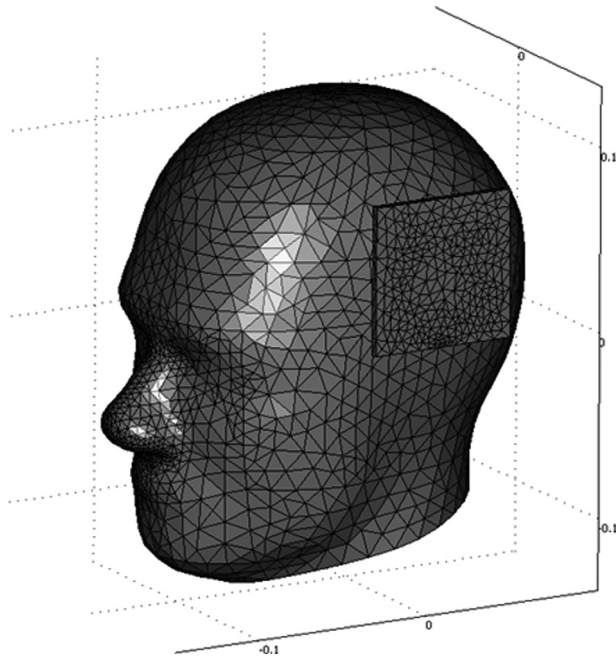


Fig. 4 A three-dimensional finite element mesh of human head model

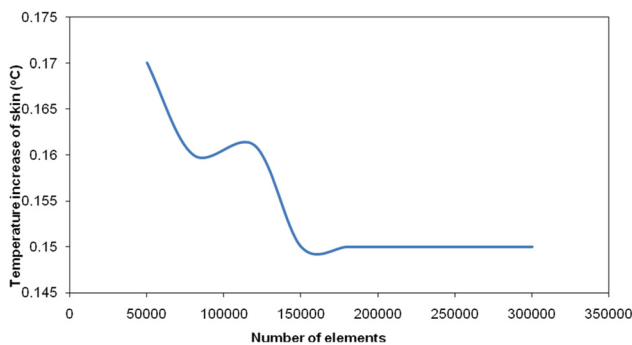


Fig. 5 Grid convergence curve of the 3D model

discretized using hexagonal elements and the Lagrange quadratic is used to approximate temperature and SAR variation across each element. Convergence tests of the frequency of 900 MHz case are carried out to identify a suitable number of elements required. The convergence curve resulting from the convergence test is shown in Fig. 5. This convergence test leads to a grid with approximately 200,000 elements. It is reasonable to assume that, with this element number, the accuracy of the simulation results is independent of the number of elements. Cases with higher numbers of elements are not tested due to a lack of computational memory and performance.

4 Results and Discussion

In this study, the mathematical model of bioheat transfer and electromagnetic wave propagation for all cases is used for the analysis. For the simulation, the dielectric and thermal properties are directly taken from Tables 2 [18] and 3 [11,19], respectively. The exposed radiated power used in this study refers to ICNIRP standard for safety level at the maximum SAR value of 2 W/kg [1]. In this analysis, the effects of user age (adult and 7 years old child) and radiated power (1.0, 1.5, and 2.0 W) on distributions of specific absorption rate and temperature profile within the human head are systematically investigated.

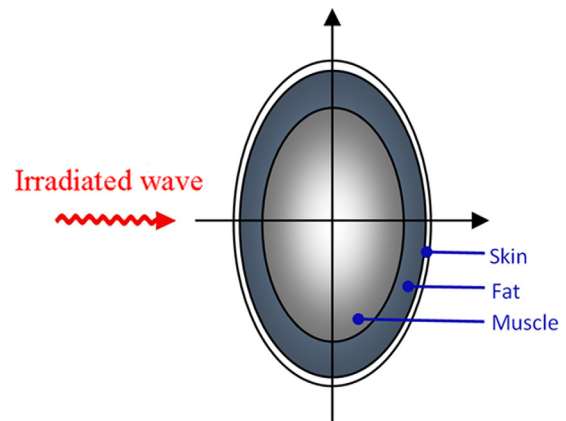


Fig. 6 Geometry of the validation model obtained from the paper

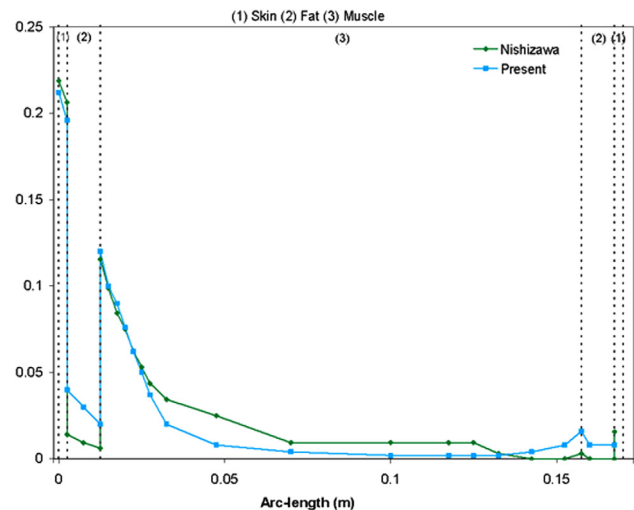


Fig. 7 Comparison of the calculated SAR distribution to the SAR distribution obtained by Nishizawa and Hashimoto [20]

Table 4 Comparison of the results obtained in the present study with those of Nishizawa and Hashimoto [20]

	Present work	Published work [20]	% Difference
SAR _{max} in skin	0.212	0.220	3.63
SAR _{max} in fat	0.198	0.206	3.88
SAR _{max} in muscle	0.116	0.120	3.33

4.1 Verification of the Model. It must be noted in advance that it is very difficult to make direct comparison of the model in this study and the experimental results because it is not possible to directly measure the temperature increase in the brain, especially in the case where the heating effect from mobile phone radiation is taken into account. In order to verify the accuracy of the present numerical model, the modified case of the simulated results is then validated against the numerical results with the same geometric model obtained by Nishizawa and Hashimoto [20]. The horizontal cross section of three layers of human tissue as shown in Fig. 6 is used in the validation case. In the validation case, the leakage power density exposed to the electromagnetic frequency of 1300 MHz is 1 mW/cm². The results of the selected test case are illustrated in Fig. 7 for SAR distribution in the human tissue. Table 4 clearly shows good agreement of the maximum value of

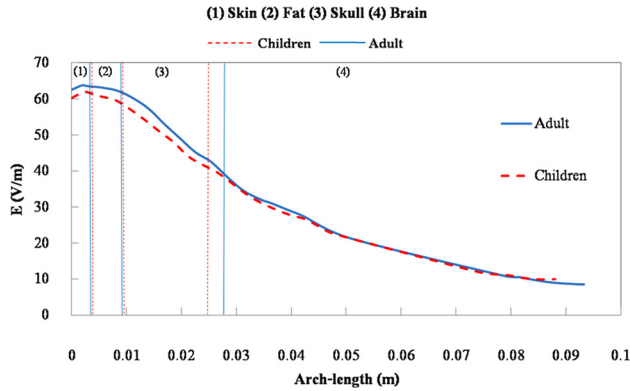


Fig. 8 Electric field distribution (V/m) in adult and child heads exposed to the radiated power of 1 W at the frequency of 900 MHz

the SAR of tissue between the present solution and that of Nishizawa. This favorable comparison lends confidence in the accuracy of the present numerical model. It is important to note that there may be some errors occurring in the simulations that are generated by the input dielectric properties and the numerical scheme.

4.2 Electric Field Distribution. A main objective of this study is to compare between the child and adult exposures from mobile phone radiation. To illustrate the distribution of penetrated electric field inside the human head, simulation analysis is required. Figure 8 shows the simulation of electric field distribution inside the child and adult heads exposed to mobile phone radiation along the extrusion line (Fig. 13(c)).

It can be seen that the higher values of electric field in both cases occur in the area of outer parts of the head, especially in skin, and fat. This is due to the different dielectric characteristics of the various tissue layers, a different fraction of the supplied electromagnetic energy will become absorbed in each layer in the human head. Consequently, the reflection and transmission components at each layer contribute to the resonance of standing wave in the human head. It can be seen that the higher values of electric field in all cases occur in the outer part area of the head, especially in skin, and fat. By comparison, the maximum electric field intensity in outer parts of the adult head displays a little higher value than that of the child head due to larger area of adult head exposed to the electric field. However, the electric field can penetrate deeper into the child head because of its small size, which results in a high specific absorption rate in tissues deep inside the child head. The electric field within the human head is extinguished where the electric field attenuates due to absorbed electromagnetic energy and is then converted to heat. The electric field diminishes within small distances, which results in a low specific absorption rate in organs deep inside the human head. This phenomenon explains why the electric field and therefore the specific absorption rate are greatest at the skin and decay sharply along the propagation direction for a short wavelength.

4.3 SAR Distribution. Figure 9 shows the SAR distribution evaluated on the horizontal section of the human head in which the maximum SAR value occurs. It is evident from the results that the dielectric properties, as shown in Table 1, can become significant to SAR distributions in human tissue when electromagnetic energy is exposed in these tissues. The magnitude of dielectric properties in each tissue will directly affect the amount of SAR within the human head. For both the adult and child heads, the maximum SAR values are always in the ear region. The highest SAR values are obtained in the region of the skin, for the adult head displays SAR of 1.585 W/kg and for the child head, 1.507 W/kg. It is found that the SAR distribution pattern in the human

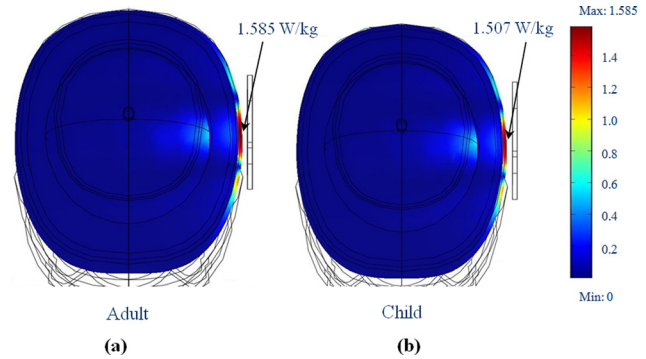
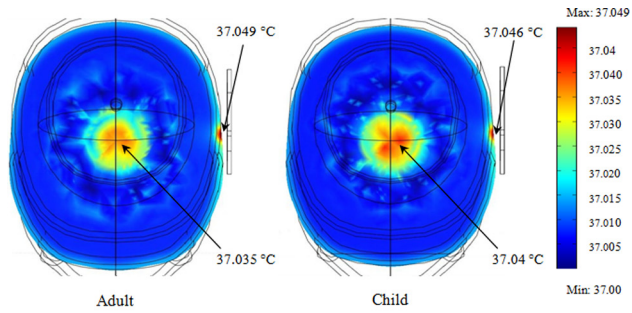


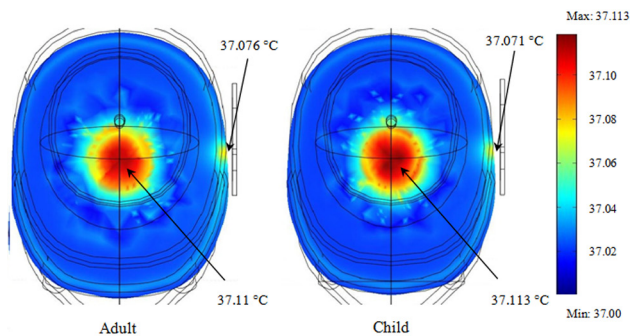
Fig. 9 SAR distribution (W/kg) in adult and child heads exposed to the radiated power of 1 W at the frequency of 900 MHz

head is depended on the effect of the dielectric properties of human tissue. With penetration into the head, the SAR values decrease rapidly along the distance. However, it can be observed that there is a deeper penetration of mobile phone radiation into the child head. This is due to the fact that the child head is smaller causing the electric field to penetrate deeper into the inner part of the head. From Fig. 9, it appears that for the child head, the higher value of SAR also occurs in the brain region due to the effect of high value of the dielectric properties. Comparing these results to the ICNIRP limit of SAR value (2W/kg), one sees that the resulting SAR from this study does not exceed the limit value in all cases.

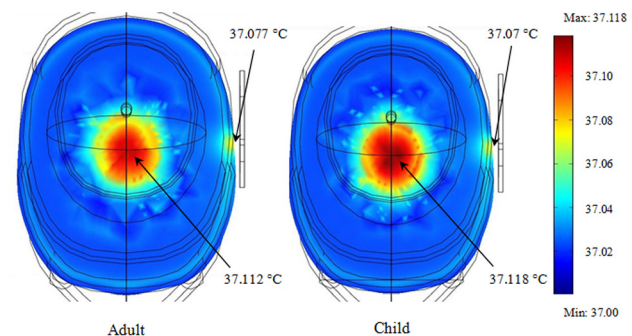
4.4 Temperature Distribution. In order to study the heat transfer within the human head, the coupled effects of electromagnetic wave propagation and unsteady bioheat transfer are investigated. Due to these coupled effects, the electric field distribution in Fig. 8 and the SAR distribution in Fig. 9 are then converted into heat by absorption of the tissues. Figure 10 shows the temperature distribution in the horizontal cross section human heads exposed to mobile phone radiation at various times. For the human head exposed to the mobile phone radiation for a period of time, the temperature within the human head (Fig. 10) is increased, according to the specific absorption rate (Fig. 9). This is because the electric field within the human head attenuates owing to the energy absorbed and thereafter the absorbed energy is converted to thermal energy, which increases the human head temperature. It is found that at the different ages of the mobile phone users, the distribution patterns of temperature at a particular time are quite different. The hot spot zone is strongly displayed at 10 min for the child head at the middle of the child head, owing to the extensive penetration of electromagnetic power of internal regions and higher dielectric properties of child tissues. The higher temperature in the brain is also resulting from the child's higher rate of metabolism. To a lesser extent, the temperature increases in the adult human head are always found at the external region of the head correlated to the electric field and SAR values (Figs. 8 and 9). After being exposed to radiation for 30 min, the highest temperature of adult and child heads occurs in the brain region of 37.112 °C and 37.118 °C, respectively, as shown in Fig. 10(c). It can be seen that the maximum temperature of the child head is higher than the maximum temperature of the adult head. One of the reasons is that the higher dielectric property of the child head has stronger absorption ability of electromagnetic radiation than that of the adult head. Moreover, the smaller size of the child head also allows the electromagnetic wave to penetrate further into the child's smaller head. The maximum temperature increases with the radiated power, for instance for each 1 W, adult and child head temperatures rise 0.112 °C and 0.118 °C, respectively. This is much lower than the thermal damage temperature of 3.5 °C [3].



(a)



(b)



(c)

Fig. 10 The temperature distribution in adult and child heads exposed to the radiated power of 1 W at the frequency of 900 MHz: (a) 1 min, (b) 10 min, and (c) 30 min

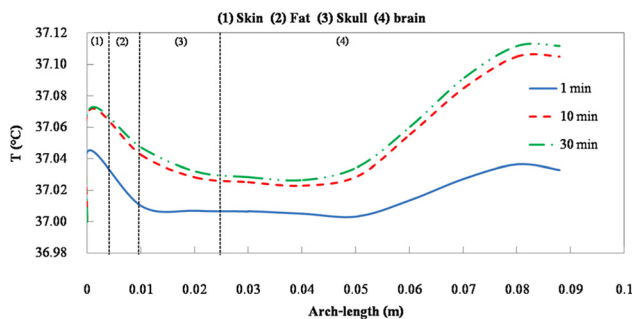


Fig. 11 Temperature distribution versus arc-length of child head at various times exposed to the electromagnetic frequency of 900 MHz at the radiated power of 1 W

A mobile phone radiation exposure usually lasts only a few minutes; hence, the steady-state temperature rise is rarely reached. Figures 11 and 12 show the temperature distributions inside adult and child heads for different exposure times. The brain has a high

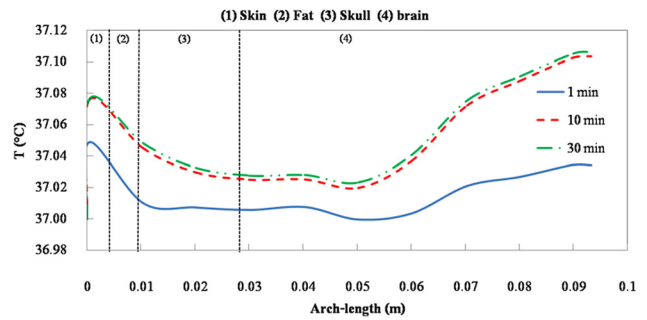


Fig. 12 Temperature distribution versus arc-length of adult head at various times exposed to the electromagnetic frequency of 900 MHz at the radiated power of 1 W

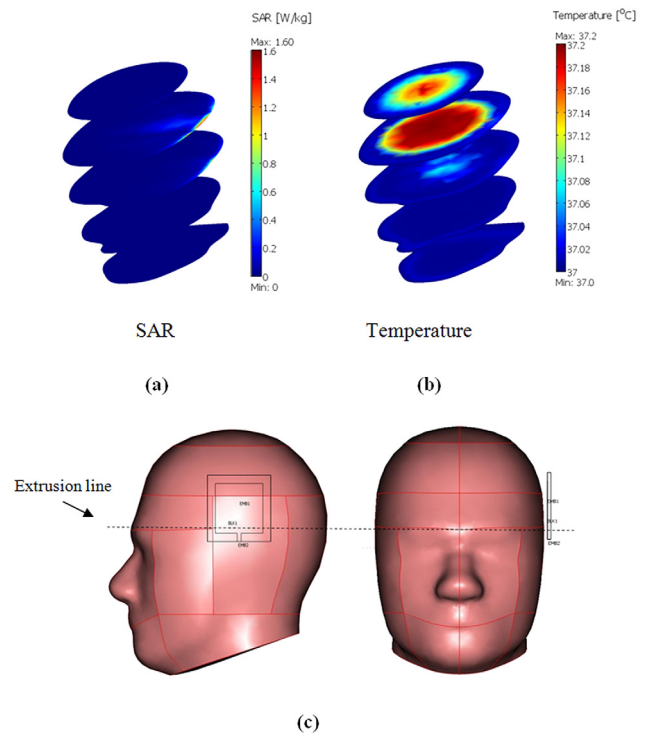


Fig. 13 The slice plot and extrusion line in the human head. Slice plot of (a) SAR distribution and (b) temperature distribution. (c) The extrusion line in the human head where the SAR and temperature distributions are considered.

metabolic heat generation rate and consequently a higher temperature than tissues with a lower rate of metabolic heat generation. For both cases, the temperature increases in the region of the skin are highest in the early time of exposure to mobile phone radiation. Surprisingly, just after 10 min of exposure, the temperature increases in the skin region are lower than that of the brain region. This is because the higher blood perfusion of the skin tissue keeps the temperature lower.

4.5 Comparison of SAR Distribution and Temperature Distribution in Human Tissues. In order to study the comparison of the SAR distribution and temperature distribution within the human head, the SAR and temperature distributions along an extrusion line as shown in Fig. 13(c) are investigated. Figures 13(a) and 13(b) show the SAR distribution and the temperature distribution of an adult head exposed to the electromagnetic frequency of 900 MHz for 30 min at the radiated power of 1 W as a slice plot. The slice plot in Figs. 13(a) and 13(b) showing the

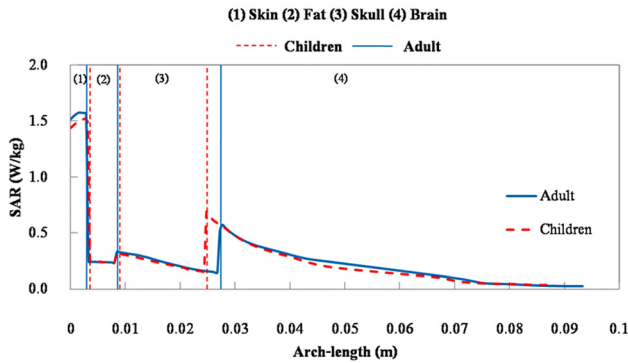


Fig. 14 SAR distribution versus arc-length of adult head and child head exposed to the radiated power of 1 W

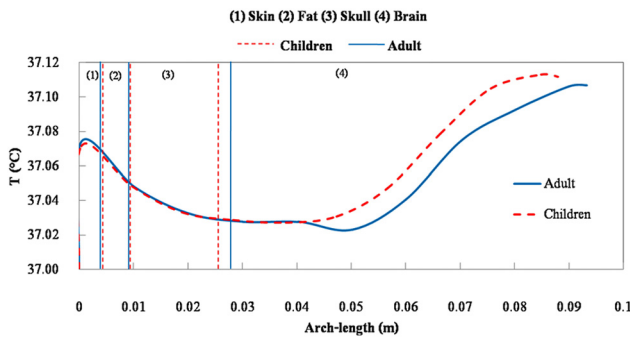


Fig. 15 Temperature distribution versus arc-length of adult head and child head exposed to the radiated power of 1 W for 30 min

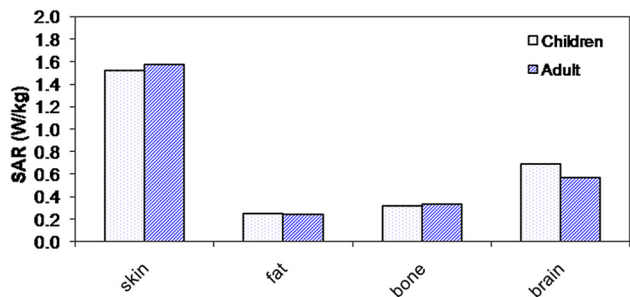


Fig. 16 Comparison of the maximum SAR in human tissues for adult and child heads

SAR and temperature distributions inside the human head gives important information. Consider the relation of SAR and temperature distributions at the extrusion line (Fig. 13(c)). Temperature increases of human tissues are induced by local dissipation of SAR. For a human head exposed to the radiated power of 1 W, Fig. 14 shows the maximum SAR of the adult head (1.5 W/kg) in the skin region. The maximum SAR value of the child head is approximately equal to the maximum SAR value of the adult head (1.5 W/kg) in the skin. The SAR value at the middle of the child head is approximately equal to the maximum SAR value of the adult head. However, Fig. 15 shows that the maximum temperature of the child head in the middle brain region (37.118 °C) is higher than the maximum temperature of the adult head in the middle brain region (37.112 °C).

As for the SAR distribution (Fig. 14), there is no significant difference between values for adults and children. However, the deviation between the temperature distribution of the adult and

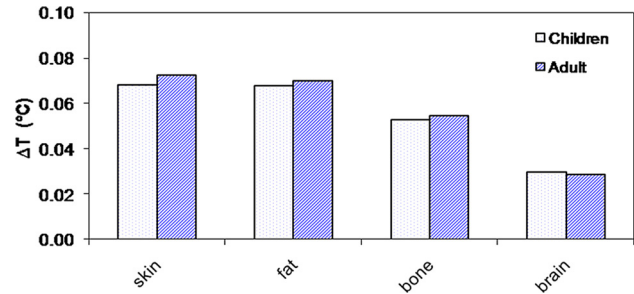


Fig. 17 Comparison of the temperature increases in human tissues for adult and child heads

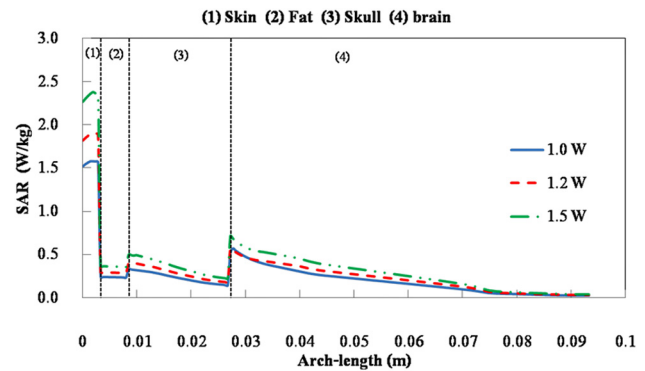


Fig. 18 SAR distribution versus arc-length of human head exposed to the electromagnetic frequency of 900 MHz at various radiated power

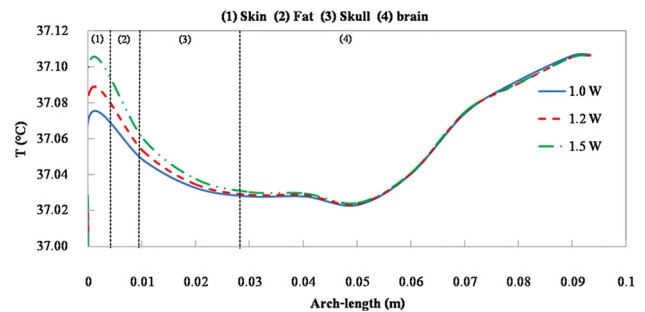


Fig. 19 Temperature distribution versus arc-length of human head exposed to the electromagnetic frequency of 900 MHz at various radiated power, at $t = 30$ min

child occurs in the middle of the head (Fig. 15). One of the reasons is that the higher dielectric property of the child brain has stronger absorption ability of electromagnetic radiation than that of the adult brain. Moreover, the smaller size of the child head also allows the electromagnetic wave to penetrate further into the child's smaller head. In addition, smaller head has lower thermal resistance than the larger counterparts. This different behavior is due to the fact that for the same SAR value at different dielectric properties, the temperature distribution is not the same (Fig. 16).

Figure 17 shows the localized maximum SAR values for the adult and child heads. For the value of localized SAR for each tissue layer, it is found that SAR distribution is related to the electric field distribution as well as the dielectric properties of the tissue. For both cases, the three highest SAR values, including skin, brain, and bone are shown. Furthermore, most of the localized SAR values of the adult head are higher than that of the child head, except the brain. This is because the electrical conductivity of child brain is particular higher than that of adult brain.

Figure 17 shows the maximum localized temperature increases in all tissues for the adult and child heads. The highest temperature increase in both cases occurs in the skin; it is observed that the second highest temperature increase in both cases appears in the fat tissue, not in the brain like the SAR values. This is because the fat tissue has a lower blood perfusion rate (4.58×10^{-4} 1/s) than that of the brain (8.83×10^{-3} 1/s). It causes the heat transfer due to blood perfusion which is less effective in fat. At the same time, there is also the contribution of heat conduction from the skin tissue which displays a strong influence on the fat temperature.

In addition, it is found that the temperature distributions are not directly proportional to the local SAR values. Nevertheless, these are also related to parameters, such as thermal conductivity, dielectric properties, blood perfusion rate, etc. It is therefore important to use a strongly coupled model for thermal and electromagnetic wave propagation to assess the health effects of exposure to electromagnetic waves.

4.6 Effect of Radiated Power. The effect of radiated power (the power radiated by the mobile phone) has also investigated. Figure 18 shows the comparison of the SAR distribution within the human head at various radiated powers, with the frequency of 900 MHz, along the extrusion line (Fig. 13(c)). Figure 19 shows the temperature distribution within the human head along the extrusion line at $t = 30$ min corresponding to radiated powers of 1.0, 1.5, and 2.0 W. It is found that mobile phone radiated power significantly influences the temperature distribution. Greater power provides greater heat generation inside the human head, thereby increasing the temperature within the human head.

5 Conclusions

This study presents the numerical simulation of SAR and temperature distributions in adult and child heads exposed to mobile phone radiation at the frequency of 900 MHz with the radiated power of 1.0, 1.2, and 1.5 W. The numerical simulations in this study show several important features of the energy absorption in the human head. Referring to SAR values, the ICNIRP limit (2 W/kg) is exceeded with respect to SAR limits in the case of using radiated power at 1.5 W. The temperature increases calculated in this study are lower than the thermal damage thresholds in all the considered situations.

The results show that the maximum temperature increases in various organs are significantly different for the different ages. The maximum temperature increase in the skin of an adult head is higher than that of child head. While the maximum temperature increase in the brain of an adult head is lower than that of child head. It is found that greater radiated power results in a greater heat generation inside the human head, thereby increasing the rate of temperature increase. Moreover, it is found that the temperature distributions in human head induced by mobile phone radiation are not directly related to the SAR distribution, due to the effects of dielectric properties, thermal properties, blood perfusion, and penetration depth of the electromagnetic power.

Therefore, health effect assessment of mobile phone radiation requires utilization of numerical simulation from an SAR model along with a thermal model. Future work will focus on the frequency-dependent dielectric properties of human tissue. A study will also develop a more realistic model for simulations and study the temperature dependency of dielectric properties. This will allow a better understanding of the realistic situation of the interaction between electromagnetic fields from mobile phone radiation and the human tissues.

Acknowledgment

This work was supported by the National Research University Project of Thailand, Office of Higher Education Commission and the Thailand Research Fund (TRF). The authors wish to express

their gratitude to Mr. Watjakorn Kunamornlert, Mr. Apichart Sasue, and Ms. Juntakan Nuraksa for their help to run the program.

Nomenclature

C = specific heat capacity (J/(kg °C))
 E = electric field intensity (V/m)
 f = frequency of incident wave (Hz)
 j = current density
 k = thermal conductivity (W/(m °C))
 n = normal vector
 Q = heat source (W/m³)
 T = temperature (K)
 t = time

Greek Symbols

μ = magnetic permeability (H/m)
 ε = permittivity (F/m)
 σ = electric conductivity (S/m)
 ω = angular frequency (rad/s)
 ρ = density (kg/m³)
 ω_b = blood perfusion rate (1/s)

Subscripts

b = blood
 ext = external
 met = metabolic
 r = relative
 0 = free space, initial condition

References

- [1] International Commission on Non-Ionizing Radiation Protection (ICNIRP), 1998, "Guidelines for Limiting Exposure to Time-Varying Electric, Magnetic and Electromagnetic Fields (up to 300 GHz)," *Health Phys.*, **74**, pp. 494–522.
- [2] IEEE, 1999, "IEEE Standard for Safety Levels With Respect to Human Exposure to Radio Frequency Electromagnetic Fields, 3 kHz to 300 GHz," IEEE Standard C95.1-1999.
- [3] Guyton, A. C., and Hall, J. E., 1996, *Textbook of Medical Physiology*, Saunders, Philadelphia, PA, Chap. 73.
- [4] Adair, E. R., Adams, B. W., and Akel, G. M., 1984, "Minimal Changes in Hypothalamic Temperature Accompany Microwave-Induced Alteration of Thermoregulatory Behavior," *Bioelectromagnetics*, **5**, pp. 13–30.
- [5] Pennes, H. H., 1998, "Analysis of Tissue and Arterial Blood Temperatures in the Resting Human Forearm," *J. Appl. Phys.*, **85**, pp. 5–34.
- [6] Yang, D., Converse, M., and Mahvi, D., 2007, "Expanding the Bioheat Equation to Include Tissue Internal Water Evaporation During Heating," *IEEE Trans. Biomed. Eng.*, **54**, pp. 1382–1388.
- [7] Okajima, J., Maruyama, S., and Takeda, H., 2009, "Dimensionless Solutions and General Characteristics of Bioheat Transfer During Thermal Therapy," *J. Therm. Biol.*, **34**, pp. 377–384.
- [8] Chua, K. J., and Chou, S. K., 2009, "On the Study of the Freeze-Thaw Thermal Process of a Biological System," *Appl. Therm. Eng.*, **29**, pp. 3696–3709.
- [9] Yang, W. J., 1989, *Biothermal-Fluid Sciences*, Hemisphere Publishing Company, Washington, D.C.
- [10] Wessapan, T., Srisawatdhisukul, S., and Rattanadecho, P., 2012, "Specific Absorption Rate and Temperature Distributions in Human Head Subjected to Mobile Phone Radiation at Different Frequencies," *Int. J. Heat Mass Transfer*, **55**, pp. 347–359.
- [11] Wessapan, T., Srisawatdhisukul, S., and Rattanadecho, P., 2011, "Numerical Analysis of Specific Absorption Rate and Heat Transfer in the Human Body Exposed to Leakage Electromagnetic Field at 915 MHz and 2450 MHz," *ASME J. Heat Transfer*, **133**, p. 051101.
- [12] Wessapan, T., Srisawatdhisukul, S., and Rattanadecho, P., 2011, "The Effects of Dielectric Shield on Specific Absorption Rate and Heat Transfer in the Human Body Exposed to Leakage Microwave Energy," *Int. Commun. Heat Mass Transfer*, **38**, pp. 255–262.
- [13] Keangin, P., Rattanadecho, P., and Wessapan, T., 2011, "An Analysis of Heat Transfer in Liver Tissue During Microwave Ablation Using Single and 2 Double Slot Antenna," *Int. Commun. Heat Mass Transfer*, **38**, pp. 757–766.
- [14] Wang, J., and Fujiwara, O., 2003, "Comparison and Evaluation of Electromagnetic Absorption Characteristics in Realistic Human Head Models of Adult and Children for 900-MHz Mobile Telephones," *IEEE Trans. Microwave Theory Tech.*, **51**, pp. 966–971.
- [15] Spiegel, R. J., 1984, "A Review of Numerical Models for Predicting the Energy Deposition and Resultant Thermal Response of Humans Exposed to Electromagnetic Fields," *IEEE Trans. Microwave Theory Tech.*, **32**(8), pp. 730–746.

- [16] Kanai, H., Marushima, H., Kimura, N., Iwaki, T., Saito, M., Maehashi, H., Shimizu, K., Muto, M., Masaki, T., Ohkawa, K., Yokoyama, K., Nakayama, M., Harada, T., Hano, H., Hataba, Y., Fukuda, T., Nakamura, M., Totsuka, N., Ishikawa, S., Unemura, Y., Ishii, Y., Yanaga, K., and Matsuura, T., 2007, "Extracorporeal Bioartificial Liver Using the Radial-Flow Bioreactor in Treatment of Fatal Experimental Hepatic Encephalopathy," *Artif. Organs*, **31**(2), pp. 148–151.
- [17] Shen, W., and Zhang, J., 2005, "Modeling and Numerical Simulation of Bioheat Transfer and Biomechanics in Soft Tissue," *Math. Comp. Model.*, **41**, pp. 1251–1265.
- [18] Wang, J., Fujiwara, O., and Watanabe, S., 2006, "Approximation of Aging Effect on Dielectric Tissue Properties for SAR Assessment of Mobile Telephones," *IEEE Trans. Electromagn. Compat.*, **48**(2), pp. 408–413.
- [19] Hirata, A., Fujimoto, M., Asano, T., Wang, J., Fujiwara, O., and Shiozawa, T., 2006, "Correlation Between Maximum Temperature Increase and Peak SAR With Different Average Schemes and Masses," *IEEE Trans. Electromagn. Compat.*, **48**(3), pp. 569–578.
- [20] Nishizawa, S., and Hashimoto, O., 1999, "Effectiveness Analysis of Lossy Dielectric Shields for a Three-Layered Human Model," *IEEE Trans. Microwave Theory Tech.*, **47**(3), pp. 277–283.